

# Pressure induced Raman and fluorescence singularities in $LiYF_4$

Qiuping A. Wang

Institut Supérieur des Matériaux du Mans,  
44, Avenue F.A. Bartholdi, 72000 Le Mans, France

Alain Bulou and Jean-Yves Gesland

Laboratoire de Physique de l'État Condens, CNRS UMR6087,  
Universit du Maine, 72085 Le Mans Cedex 9, France

## Abstract

The pressure effect on the fluoride scheelite laser host  $LiYF_4$  is studied at room temperature up to 26 GPa by Raman scattering and up to 40 GPa by  $P^{3+}$  fluorescence of doped sample. The Raman spectra exhibit three singularities at the vicinity of 6 GPa, 10-12 GPa and 16-17 GPa. The samples pressurized to 21 GPa or higher do not recover the original phase after being released, giving more Raman lines than original samples. The luminescence spectra of  $P^{3+}$  are collected in the energy range corresponding to following transitions  $^3P_{0,1} - ^3H_{4,5,6}$ ,  $^1D_2 - ^3H_4$  and  $^3P_0 - ^3F_2$ . Singularities are observed in the vicinity of 6 GPa, 10 GPa, 16 GPa, 23 GPa in agreement with the Raman study. Moreover, an irreversible transition occurs at 23 GPa. The samples pressurized to above 26 GPa become amorphous when released and all the sharp lines disappear. Above 31 GPa, the spectra at high pressures show only some broad bands corresponding to transitions between two multiplets of the  $^4F_2$  configuration of  $Pr^{3+}$ . These singularities suggest possible phase transformations leading to lowering of the lattice symmetry.

PACS numbers : 64.70.Kb; 62.50.+p; 78.30.Hv

# 1 Introduction

$LiYF_4$  doped with rare earth ions such as  $Nd^{3+}$  and  $Pr^{3+}$  is a well known laser material with the tetragonal scheelite structure (Figure 1 and 2) which is known to be one of the rare crystal families undergoing ferroelastic phase transition with temperature and pressure[1, 2, 3, 4, 5, 6]. At ambient condition, this crystal has  $C_{4h}^6$  space group. Recently, the lattice dynamics of  $LiYF_4$  has been well studied theoretically and experimentally with IR absorption, Raman and neutron scattering[7, 8, 9, 10]. The crystal structure of  $LiYF_4$  is relatively stable in temperature, no transition being observed from 10 K to 1000 K[7, 11]. But phase transformations under high pressures have been shown to be possible by Raman and luminescence studies[11, 12]. These works, especially those under high pressures, are very helpful for understanding the dynamics of this lattice and for the verification of the validity of the rigid ion models employed in the dynamical calculations.

In a Raman study under pressure up to 20 GPa[11], a sudden change in the Raman frequency slope  $\frac{\partial\omega}{\partial P}$  was observed around 7 GPa and attributed to the stiffening of  $LiF_4$  tetrahedra. No anomaly was noted above this pressure. Due to the ambiguity of mode assignment for high pressure Raman frequencies, the result of this work is not unquestionable.

$LiYF_4$  doped with rare earth ions gives often very intense emission[14]. Each rare earth ion is coordinated to eight F-ligand ions, getting the site symmetry  $D_{2d}$  or  $S_4$  (figure 1). It is expected that the luminescence spectra of rare earth ions are very sensible to the behavior (rotation or deformation) of  $LiF_4$  tetrahedra under pressure. A work on  $Eu^{3+} : LiYF_4$  has been carried out up to 15 GPa and led to the conclusion that a phase transition was possible at 10 GPa due to the splitting of some Stark levels meaning lowering of site symmetry of  $Eu^{3+}$ .

In this paper, we present the results of the study of  $Pr^{3+} : LiYF_4$  with both Raman and Luminescence.  $Pr^{3+}$  in  $LiYF_4$  gives very sharp luminescence lines in the visible spectral region with clear line assignments[13, 14, 15, 16, 17]. It was expected that the study can be carried out at much higher pressures than in previous works and gives us more information about the lattice behavior under pressure. Our pressure has reached 40 GPa. Several singularities in Raman and luminescence spectra have been observed. It is concluded that phase transitions induced by pressure are indeed possible.

## 2 Raman study

### 2.1 Experiment and result

The samples are small single crystals of  $LiYF_4$  of about 100  $\mu m$  width and 50  $\mu m$  thick. The pressure was generated with a gasketed diamond anvil cell

Diacell MK3 with a pair of anvils of type IIb/a diamond (0.16 carat) mounted upon tungsten carbide support plates. The anvil flats are  $550\text{ }\mu\text{m}$  in diameter. The gasket in Inconel was indented before drilling a hole (pressure chamber) in the centre of the indentation. The cylindrical pressure chamber is  $100\text{ }\mu\text{m}$  in diameter and less than  $100\text{ }\mu\text{m}$  high. A chip of the sample is put into the pressure chamber together with a small ruby (for pressure measurement) and the pressure medium consisting of a 4:1 mixture of methanol:ethanol. Pressure calibration is carried out by the shift of the R lines of ruby with the non-linear pressure scale[18]. The Raman spectra are excited by the  $514.5\text{ nm}$  line of an argon ion laser with  $130\text{ mW}$  total power measured just before the first anvil and collected through the type IIb anvil with a Dilor-Z24 triple-monochromator single channel Raman spectrometer. The spectra are recorded under microscope with different orientations of the sample in the pressure chamber in order to obtain as many Raman lines as possible with different polarisations (since polarization analysis is difficult in the pressure cell). Above  $21\text{ GPa}$ , the Raman signals of the samples submitted to monotonic pressure increase become so weak that they could not be observed even with a very long photon counting time (20 scans of 2 seconds). However, it was found that better signals were obtained if we used again the samples released from high pressure lightly above  $10\text{ GPa}$ . Under this condition, Raman signals were observed up to  $26\text{ GPa}$ .

High pressure Raman spectra are shown in Figure 3. We have observed more lines at low frequency than the previous work[11]. The 13 expected lines at ambient pressure give rise to 9 bands as expected due to frequency overlaps[7, 8, 9, 10]. Frequency splitting occurs under small pressure increase so that 12 lines can be clearly identified (the missing line overlaps the low frequency of  $E_g$  line and does not give significant signal. Their frequencies are reported in Table 1. The significant variation in the intensity of some lines in the range of  $10\text{-}14\text{ GPa}$  mainly results from the orientation change of the samples in the pressure chamber during the experiments. The pressure dependence of the Raman frequencies is plotted in Figure 4. The frequencies of all modes but one increase with increasing pressure with singularities at roughly  $6\text{ GPa}$ ,  $10\text{ GPa}$  and  $17\text{ GPa}$ .

## 2.2 Discussion of Raman results

### 2.2.1 Preliminary remarks

Before analyzing the singularities in details, it is useful to give some information about the structure and its characteristic parameters. The pressure effect mainly results in a contraction of the crystal, proportional to the elastic constants  $S_{11}$  and  $S_{33}$ . According to reference[19] these constants are  $12.8\text{ GPa}^{-1}$  and  $7.96\text{ GPa}^{-1}$ , respectively, which means that the crystal will un-

dergo greater contraction along the **a** parameter than along the **c** parameter. From the microscopic point of view, the Li-F and Y-F distance are 1.902 Å and 2.286 Å, respectively, while the shortest sums of the ionic radii are respectively 1.88 Å and 2.30 Å[20]. Similarly the shortest F-F distances in  $LiF_4$  and  $YF_8$  polyhedra are respectively 2.984 Å and 2.815 Å, while the sum of the ionic radii is 2.57 Å. This suggests that the contraction of the crystal lattice will result mainly in the reduction or deformation of  $LiF_4$  polyhedra. Finally, it appears from figure 2 that an increase of the angle of the rotation of the  $LiF_4$  tetrahedra around the tetragonal axis should decrease the parameter **a**, provided the tetrahedra undergo a distortion in order not to shorten the Li-F distance. So it is expected that increasing pressure would preferably result in a decrease of **a**, a decrease of the Li-F bond lengths and an increase of the rotation angle of  $LiF_4$  tetrahedra around the **c** axis.

### 2.2.2 Singularities at 6 GPa

As observed in the previous work[11], the first singularity around 6 GPa mainly consist in the splitting of the Bg/Eg lines in the vicinity of 350  $cm^{-1}$  and 400  $cm^{-1}$  (the splitting becomes 65  $cm^{-1}$  for the former and 17  $cm^{-1}$  for the latter at 17 GPa) and a sudden change in the pressure dependence of the modes at about 350  $cm^{-1}$  and 460  $cm^{-1}$ ; the latter corresponds to the stretching of  $LiF_4$  tetrahedron[8]. We think that a simple stiffening (without other modifications) of  $LiF_4$  tetrahedra due to pressure would not be sufficient to account for the abrupt slope change which suggests some modifications in the structural characteristics (with or without symmetry change). A plausible hypothesis is a sudden rotation of  $LiF_4$  tetrahedra towards the limit value  $\phi = 45^\circ$  due to the contraction of the lattice along **a** (cf. Figure 2). Note that the decrease of the rotation angle from  $\phi = 29^\circ$  to  $\phi = 0^\circ$ . (leading to zircon structure) would require the increase of parameter **a** and so cannot be considered. In this case of unchanged symmetry, the line splitting is simply the separation of the overlapped Eg and Bg modes at ambient pressure, as is observed in the work of the reference[9] for the series  $LiXF_4$  (X=Y, Ho, Er, Tm, Yb). Another possible interpretation is that it is associated with a symmetry change so the observed line splitting would rather be a splitting of the Eg modes. This idea is supported by the fact that a splitting of the luminescence lines of  $Pr^{3+}$  in  $LiYF_4$  is also observed in this pressure range (see following section).

### 2.2.3 Singularities at 10 GPa

A second singularity is observed in the vicinity of 10 GPa. There is discontinuity in the pressure shift of the frequency of the lines located at about 180  $cm^{-1}$ , 300  $cm^{-1}$  and 350  $cm^{-1}$  (see Figure 4). We should emphasize here that a splitting of the luminescence lines of  $Pr_{3+}$  in  $LiYF_4$  is also observed in the

vicinity of this pressure. In addition, we have recorded at ambient pressure the Raman spectra of the samples released from pressure of about 11 GPa. The spectrum measured immediately after the releasing (spectrum c in Figure 5) is very different from the original one (spectrum a in figure 5). Two strong additional lines are observed at  $123\text{ cm}^{-1}$  and  $580\text{ cm}^{-1}$ . All the lines are very broad, which suggests a partially amorphous state. This spectrum disappears after roughly 15 minutes for a crystal of about  $10\text{ }\mu\text{m}$  thick and  $50\text{ }\mu\text{m}$  width which recovers the original Raman lines (spectrum b in Figure 5). Since the structure above 6 GPa is not known, no mechanism can be proposed for this structure transformation. As a matter of fact, any of the mechanisms proposed to explain the singularities at 6 GPa is possible in the structural change at 10 GPa.

#### 2.2.4 Singularities at 17 GPa

A third singularity appears at about 17 GPa. It is mainly characterized by the vanishing of some lines between  $400\text{ cm}^{-1}$  and  $450\text{ cm}^{-1}$ , the emergence of a new line at  $435\text{ cm}^{-1}$ , a change of the pressure dependence of the frequency of the Ag mode at about  $315\text{ cm}^{-1}$ , and the existence of a minimum of the low frequency Eg mode (at  $154\text{ cm}^{-1}$ ). At higher pressure, the energy of this mode increases again with a larger shift rate than below 17 GPa and reaches  $156\text{ cm}^{-1}$  at 26 GPa. The most striking fact is that the Raman spectra (spectrum d in figure 5) recorded at ambient pressure of the samples released from 21 GPa remain definitely different from those of the sample never pressurized. This means that an irreversible transformation has occurred. Note that the frequencies of the new spectrum (d in figure 5) are close to those of the samples released from 11 GPa (c of figure 5).

The irreversibility and the significant change of the high pressure Raman spectra suggest that this very high pressure phase transformation would be reconstructive. However, as previously pointed out, it seems to be associated with a softening of the low frequency Eg mode, as would occur for a second order (reversible) phase transition. This can be seen in figure 6 where the square of the frequency is plotted against pressure, giving following relationship :

$$\omega^2 = A(p - p_0) \quad (1)$$

for  $P < 17\text{ GPa}$ , where  $A = 300\text{ cm}^{-2}\text{GPa}^{-1}$  and  $p_0 = 80\text{ GPa}$ ; and :

$$\omega^2 = A'(p'_0 - p) \quad (2)$$

for higher pressure with  $A' = 794\text{ cm}^{-2}\text{GPa}^{-1}$  and  $p'_0 = -7\text{ GPa}$ .

In this framework, this phase transition would be a proper ferroelastic one since the soft mode, observed below and above the transition, has the same symmetry as a strain tensor[1]. It is worth noticing that, due to its degeneracy,

it would be associated with the existence of a soft acoustic plane [21], a kind of transition expected but never experimentally observed to our knowledge. We recall that the scheelite  $BiVO_4$  undergoes also a proper ferroelastic phase transition in which the softening of an acoustic branch was observed. But the soft mode has a one dimensional Bg symmetry. The values of A and A' for  $LiYF_4$  are about three times smaller than those for  $BiVO_4$ , but  $(A'/A) = 2.61 \pm 0.5$  for  $LiYF_4$  is very close to  $(A'/A) = 2.67 \pm 0.2$  observed for  $BiVO_4$  [4]. What is really questionable is the fact that such a transition, clearly associated to a soft mode, is irreversible. Actually a similar phenomenon has already been observed in the layered tetrafluoroaluminate  $KAlF_4$  in which an irreversible martensitic phase transition appears after the softening of a flat Brillouin zone boundary phonon branch [22]. So, the softening of the low frequency Eg mode may be associated with a similar mechanism.

### 3 Luminescence study

#### 3.1 Experimental results

The technical details of the pressure experiment are described in the above section. The sample is  $LiYF_4$  single crystal doped with approximately 1 mol  $Pr^{3+}$ . The fluorescence spectra are excited at 457.9 nm with an argon ion laser. The pressure goes up to 40 GPa and the emission spectra are recorded in the range  $15000\text{ cm}^{-1}$ – $21500\text{ cm}^{-1}$  corresponding to the transitions from  $^3P_0$ ,  $^3P_1$  and  $^1D_2$  initial states to  $^3H_4$ ,  $^3H_5$ ,  $^3H_6$  and  $^3F_2$  final states.

The observed lines at ambient pressure are summarized in Table 2. The assignments of the transitions are given for  $S_4$  site symmetry of the  $Pr^{3+}$  ion [13, 15]. Twenty four emission lines ( $L_1$  to  $L_{24}$ ) are assigned to the transitions between five initial states and fourteen final ones. The  $^3H_5$  level at  $2673\text{ cm}^{-1}$  was not observed before and is determined in this work by two sharp lines at  $18197\text{ cm}^{-1}$  (from  $^3P_0$ ) and  $18752\text{ cm}^{-1}$  (from  $^3P_1$ ). It is assigned to  $\Gamma_{3,4}$  symmetry according to the calculated result of reference [15].

The pressure effect on the observed fluorescence spectra is shown in figure 7. In figure 8 is plotted the pressure shift of the observed emission lines. It can be seen that, in spite of some vanishing lines, the number of the emission lines increases constantly up to 31 GPa at which all the lines abruptly vanish. The remaining spectra contain only some broad emission bands showing a weak pressure shift up to 40 GPa. Briefly, singularities are observed at 6 GPa (26 lines), 10 GPa (32 lines), 16 GPa (34 lines), 23 GPa (37 lines) and 31 GPa (vanishing of all the lines). They will be discussed below in detail.

## 3.2 Discussion of fluorescence results

### 3.2.1 Singularity at 6 GPa

The first singularity occurs at 6 GPa as in Raman spectra. Two strong lines ( $L_7$  and  $L_8$ ) from the transitions  ${}^3P_1(\Gamma_{3,4})$ - ${}^3H_5(\Gamma_2)$  and  ${}^3P_1(\Gamma_{3,4})$ - ${}^3H_5(\Gamma_{3,4})$  vanish (figure 8b) and two additional lines at  $18590\text{ cm}^{-1}$  ( $L_{n1}$ ) and  $15530\text{ cm}^{-1}$  ( $L_{n2}$ ) are observed.  $L_{n1}$  cannot be interpreted by the splitting of the  $18592\text{ cm}^{-1}$  line ( $L_9$ ) from the transition  ${}^3P_0(\Gamma_1)$ - ${}^3H_5(\Gamma_2)$  between two singlets. It could be attributed to the transitions  ${}^3P_0(\Gamma_1)$ - ${}^3H_5(\Gamma_{3,4})$ , situated at  $8\text{ cm}^{-1}$  above  $L_9$  and observed at low temperature[9,10]. That means that the appearance of  $L_{n1}$  is only a pressure induced separation between two lines close to each other.

$L_{n2}$  in figure 8d seems to be the result of a splitting of the line  $L_{21}$  from the transition  ${}^3P_0(\Gamma_1)$ - ${}^3F_2(\Gamma_{3,4})$  which is broadened before splitting, as shown in figure 7b. However it is difficult to conclude that this comes from the lifting of the degeneracy of the  ${}^3F_2(\Gamma_{3,4})$  level in a lower site symmetry, since no splitting of other levels of  $\Gamma_{3,4}$  symmetry was observed at this pressure. As a matter of fact,  $L_{n2}$  could be related to one of the transitions  ${}^3P_0(\Gamma_1)$ - ${}^3F_2(\Gamma_{3,4})$  and  ${}^3P_0(\Gamma_1)$ - ${}^3F_2(\Gamma_2)$  with the latter situated at  $20\text{ cm}^{-1}$  above the former and much less intense than the former at ambient pressure[9]. In this case, the observed splitting of  $L_{21}$  could be only the effect of different pressure dependence of two lines that fortuitously overlap at ambient pressure.

According to the above discussion, it is not sure that the singularity observed at 6 GPa are induced by a phase transition.

### 3.2.2 Singularity at 10 GPa

The singularity in the Raman spectra observed at this pressure is only a weak variation in the shift rate of the Raman mode as a function of pressure. In fluorescence, as shown in figure 8c, following additional lines are observed :  $L_{n3}$  ( $19140\text{ cm}^{-1}$ ),  $L_{n4}$  ( $19020\text{ cm}^{-1}$ ),  $L_{n5}$  ( $17100\text{ cm}^{-1}$ ),  $L_{n6}$  ( $16400\text{ cm}^{-1}$ ) and  $L_{n7}$  ( $16300\text{ cm}^{-1}$ ). A line ( $L_{19}$ ) vanishes. The slope of  $L_5$ ,  $L_{12}$ ,  $L_{13}$ ,  $L_{14}$ ,  $L_{21}$  and  $L_{23}$  abruptly changes.

$L_{n4}$  emerges in the neighborhood of a strong line  $L_5$  from the transition  ${}^3P_1(\Gamma_{3,4})$ - ${}^3H_5(\Gamma_2)$ . This looks like the splitting of the  ${}^3P_1(\Gamma_{3,4})$  level. But as seen in figure 8a, the lines  $L_1$  and  $L_2$  of the transitions  ${}^3P_1(\Gamma_{3,4})$ - ${}^3H_4(\Gamma_2)$  and  ${}^3P_1(\Gamma_{3,4})$ - ${}^3H_4(\Gamma_{3,4})$  respectively do not split. So  $L_{n3}$  and  $L_{n4}$  are probably due to the transitions from  ${}^3P_1(\Gamma_{3,4})$  to two of the levels close to  ${}^3H_5(\Gamma_2)$  at  $2280\text{ cm}^{-1}$ , i.e. the levels at  $2253\text{ cm}^{-1}$  ( $\Gamma_1$ ),  $2272\text{ cm}^{-1}$  ( $\Gamma_{3,4}$ ) and  $2297\text{ cm}^{-1}$  ( $\Gamma_1$ ) (values at ambient pressure), which were not observed at ambient pressure [9].

$L_{n6}$  and  $L_{n7}$  are close to  $L_{18}$  from the transition  ${}^3P_0(\Gamma_1)$ - ${}^3H_6(\Gamma_{3,4})$ , but none of them seems to be the result of the splitting of the  ${}^3H_6(\Gamma_{3,4})$  final state. In addition, another  ${}^3P_0(\Gamma_1)$ - ${}^3H_6(\Gamma_{3,4})$  transition ( $L_{17}$ ) remains unchanged. So

more probably  $L_{n6}$  and  $L_{n7}$  result from the transitions from  ${}^3P_0(\Gamma_1)$  to  ${}^3H_6(\Gamma_1)$  ( $4430\text{ cm}^{-1}$ ) and  ${}^3H_6(\Gamma_1)$  ( $4486\text{ cm}^{-1}$ ) in the neighborhood of  ${}^3H_6(\Gamma_{3,4})$  at  $4456\text{ cm}^{-1}$  at ambient pressure[9]. It should be noted that the transitions from  ${}^3P_0(\Gamma_1)$  to  ${}^3H_6(\Gamma_1)$  and  ${}^3H_6(\Gamma_1)$  are forbidden by the electric-dipole selection rules in  $S_4$  site symmetry[9,10].

Another singularity at this pressure is related to a sharp line at  $19260\text{ cm}^{-1}$  (see figure 8b). It cannot be attributed to any transition between the electronic or vibronic states[9-12]. It becomes very weak at about 10 GPa and rapidly disappears in the broad band of the  ${}^3P_1(\Gamma_{3,4})$ - ${}^3H_5(\Gamma_2)$  emission, as shown in figure 7a.

To conclude, a structure transformation must be invoked to explain the changes in the emission spectra, a structural modification leading to the change of transition probability and selection rules in the  $S_4$  site. This supports the suggestion of the previous work [12] and our Raman result that the ambient pressure spectrum of the samples released from 11 GPa was different from that of the scheelite structure  $LiYF_4$ .

### 3.2.3 Singularity at 16 GPa

We recall that a minimum of a pressure induced soft Raman E mode has been observed around this pressure. In fluorescence, three additional lines  $L_{n8}$  ( $18560\text{ cm}^{-1}$ ),  $L_{n9}$  ( $18470\text{ cm}^{-1}$ ) and  $L_{n10}$  ( $15470\text{ cm}^{-1}$ ) appear and two lines  $L_{20}$  and  $L_{23}$  vanish.

$L_{n8}$  and  $L_{n9}$  appear between  $L_9$  and  $L_{n1}$ , and become two sharp lines up to 30 GPa (figure 7a). Their pressure shift being almost parallel to those of the neighbouring lines (figure 8b), they could be integrated into the  ${}^3P_0$ - ${}^3H_5$  line group and attributed to the transitions from  ${}^3P_0$  to two of the three states  ${}^3H_5(\Gamma_1)$ ,  ${}^3H_5(\Gamma_{3,4})$  and  ${}^3H_5(\Gamma_1)$ , situated at ambient pressure at  $2253\text{ cm}^{-1}$ ,  $2272\text{ cm}^{-1}$  and  $2297\text{ cm}^{-1}$  respectively[9]. It should be noticed that, together with  $L_{n8}$  and  $L_{n9}$ , there are now seven observed lines in the  ${}^3P_0$ - ${}^3H_5$  group, which exceeds the number (five) of the transitions allowed by the electric-dipole selection rules in  $S_4$  site symmetry[9,10].

$L_{n10}$  is in the  ${}^3P_0$ - ${}^3F_2$  line group (figure 8d) and could only be considered as a transition from  ${}^3P_0(\Gamma_1)$  to one of the  ${}^3F_2$  levels resulting from the splitting of the  ${}^3F_2(\Gamma_{3,4})$  level, or to the fourth Stark level of  ${}^3F_2$  multiplet situated at  $5159\text{ cm}^{-1}$  ( $\Gamma_1$ ) to which the transition from  ${}^3P_0(\Gamma_1)$  is forbidden in  $S_4$  symmetry at ambient pressure. In any case, the appearance of  $L_{n10}$  suggests a change in the site symmetry of  $Pr^{3+}$ . According to Raman spectra, this transition would be a second order one.

### 3.2.4 Singularity at 23 GPa

At 23 GPa, nine additional lines emerge. They are  $L_{n11}$  ( $20709\text{ cm}^{-1}$ ),  $L_{n12}$  ( $20609\text{ cm}^{-1}$ ),  $L_{n13}$  ( $20489\text{ cm}^{-1}$ ),  $L_{n14}$  ( $18995\text{ cm}^{-1}$ ),  $L_{n15}$  ( $18596\text{ cm}^{-1}$ ),  $L_{n16}$



(16580  $cm^{-1}$ ),  $L_{n17}$  (16460  $cm^{-1}$ ),  $L_{n18}$  (16425  $cm^{-1}$ ),  $L_{n19}$  (16275  $cm^{-1}$ ) and  $L_{n20}$  (15510  $cm^{-1}$ ). On the other hand,  $L_6$ ,  $L_{13}$ ,  $L_{18}$ ,  $L_{24}$ ,  $L_{n5}$  and  $L_{n10}$  vanish (figure 8).

$L_{n11}$ ,  $L_{n12}$  and  $L_{n13}$  are in the  ${}^3P_0$ - ${}^3H_4$  group and can only be attributed to the transitions from  ${}^3P_0$  to three  ${}^3H_4$  levels in the energy range 0-300  $cm^{-1}$  (see figure 8a) just above the  ${}^3H_4(\Gamma_2)$  ground state. This, together with  $L_3$  and  $L_4$ , gives rise to five energy levels in this region where only four levels should be observed in the  $S_4$  site symmetry, namely  ${}^3H_4(\Gamma_2)$ ,  ${}^3H_4(\Gamma_{3,4})$  and two  ${}^3H_4(\Gamma_1)$ [9]. So it is reasonable to suppose that the degenerate  ${}^3H_4(\Gamma_{3,4})$  level splits into two levels giving rise to  $L_{n11}$  and the remaining  $L_4$ . This splitting should exist also in the  ${}^3P_1$ - ${}^3H_4$  group ( $L_1$  and  $L_2$ ) but unfortunately it is not possible to be observed due to the extreme signal weakness at high pressure.

Above 23 GPa, together with  $L_{n15}$ , there are eight observed lines in the  ${}^3P_0$ - ${}^3H_5$  (figure 8b) group and nine in the  ${}^3P_0$ - ${}^3H_6$  group (figure 8c) while only seven lines are allowed for the latter in  $S_4$  symmetry[9,10].

Finally, in the  ${}^3P_0$ - ${}^3F_2$  group (figure 8d), together with  $L_{n17}$ , five lines are observed, exactly the number of states in this multiplet. This means that all the energy levels are singlet at this pressure.

Another significant phenomenon is that, as in our Raman study, the luminescence of the samples released from this pressure are different from that of the samples never pressurized (Figure 9).

### 3.2.5 Singularity at 31 GPa

In the pressure range above 23 GPa, the sharp lines still exist up to 31 GPa, a pressure at which all the lines suddenly disappear (figure 7 and 8). Each of the broad bands corresponds to a transition from  ${}^3P_0$  or  ${}^3P_1$  to one of the multiplets  ${}^3H_{4-6}$  and  ${}^3F_{2-4}$ . The spectra remain the same up to 40 GPa with only a small pressure red shift of the broad bands (see figure 7 and 8). This means that the lattice of  $LiYF_4$  becomes amorphous above 31 GPa.

Similarly to the samples pressurized to above 23 GPa, the samples released from pressures higher than 31 GPa remain definitely amorphous at normal pressure, giving only broad luminescence bands as shown in Figure 7.

## 4 Final comment

In summary, we have presented in this paper the experimental results of pressure studies of  $LiYF_4$  structure by both Raman scattering and  $Pr^{3+}$  luminescence. The pressure runs up to 40 GPa. This work gives us more information about the behaviors of the lattice structure of  $LiYF_4$  than the previous ones[11, 12]. The Raman and fluorescence results are in agreement concerning the pressure effect on the structure of  $LiYF_4$ . Singularities are observed in

the vicinity of 6 GPa, 10 GPa, 16 GPa, 23 GPa and 31 GPa. Most of these singularities suggest that a simple stiffening of the lattice or the tetrahedra is not sufficient to account for the pressure evolution of the spectra and that the scheelite type structure may undergo a series of transformations or distortions responsible for the lowering of the site symmetry and the singularities at 10 GPa, 16 GPa, 23 GPa and 31 GPa. The transformations at 23 GPa and 31 GPa are irreversible, leading to amorphous structures. Of course, further work such as high pressure X-ray diffraction is necessary to clarify the situation.

With regard to the mechanism of the possible structure transformations of  $LiYF_4$  under high pressure, no precision can be given for the time being. But any of the mechanisms including the rotation and displacement of the  $LiF_4$  tetrahedra could be invoked. It is worth noticing that the internal binding of the  $LiF_4$  tetrahedra is not entirely different in comparison with the external binding[12,13], i.e. the ionic Li-F and F-F forces in the tetrahedra are of similar magnitude to the ionic Y-F and F-F forces outside the tetrahedra. So when there is a lattice distortion, we should not exclude the possibility of the distortion of the tetrahedra and of the emergence of new kinds of polyhedra under very high pressure.

## References

- [1] A. Bulou, M. Rousseau and J. Nouet, *Diffusionless Phase transitions and related structures in Oxides*, (Edited by C. Boulesteix, Trans Tech Publications, 1992), p.133
- [2] M. Wada, Y. Nakayama, A. Sawada, S. Tsunekawa and Y. Ishibashi, *J. Phys. Soc. Japan*, **47**(1979)1575
- [3] A. Pinczuk, B. Welber and F.H. Dacol, *Solid State Communication*, **29**(1979)515
- [4] A. Pinczuk, Gerald Burns and F.H. Dacol, *Solid State Communication*, **24**(1977)163
- [5] W.I.F.David and A.M. Glazer, *Phase Transitions*, **1**(1979)155
- [6] Gu Benuyan, M. Copic, and H.Z. Cummins, *Phys. Rev.B*, **24**(1981)4098
- [7] S. Salaün, M.T. Fornoni, A. Bulou, M. Rousseau, P. Simon, and J.Y. Gesland, *J. Phys. : Condens. Matter*, **9**(1997)6941  
S. Salaün, A. Bulou, M. Rousseau, B. Hennion, and J.Y. Gesland, *J. Phys. : Condens. Matter*, **9**(1997)6957  
S. Salaün, *Thèse de Doctorat de l'Université du Maine*, , Le Mans, France, 1996

- [8] S. A. Miller, H. E. Rast, and H.H. Caspers, *J. Chem. Phys.*,**52**(1970)4172
- [9] M. Fornoni, A. Bulou, J. M. Breteau, J.Y. Gesland, and M. Rousseau, *Applied Optics*,**29**(1990)1758
- [10] A. Sen, S.L. Chaplot, and R. Mittal, *Phys. Rev. B*,**64**(2001)024304
- [11] E. Sarantopoulou, Y.S. Raptis, E. Zouboulis, and C. Raptis, *Phys. Rev. B*,**59**(1999)4154
- [12] S.X. Liu, Y.B. Chi, X.Y. Zhao, L.Z Wang, *Journal of Alloys and Compounds*,**255**(1997)1-4
- [13] J.L. Adam; W.A. Sibley, and D.R. Gabbe, *Lumines.*,**33**(1985)391
- [14] C.K. Jayasankar, M.F. Reid and F.S. Richardson, *Phys. Stat. Sol. (b)*,**155**(1989)559
- [15] L. Esterowitz, F.J. Bartoli, R.E. Allen, D.E. Wortman, C.A. Morrison, and R.P. Leavitt, *Phys. Rev. B*,**219**(1979)6442
- [16] G.M. Renfro, J.C. Windscheif and W.A. Sibley, *J. Lumines.*,**212**(1980)51
- [17] H.H. Caspers and H.E. Rast, *J. Lumines.*,**10**(1975)347
- [18] H. K. Mao and P. M. Bell, *Science*,**200**(1978)1145
- [19] P. Blanchfield and G.A.Saunders, *J. Phys. C: Solid State Phys.*,**12**(1979)4673
- [20] R. D. Shannon, *Acta Cryst.*,**A32**(1976)751
- [21] R.A. Cowley, *Phys. Rev.B*,**13**(1976)4877
- [22] A. Bulou, A. Gibaud, M. Debieche, J. Nouet, B. Hennion and D. Petit-grand, *Phase Transitions*,**14**(1989)47

## Table and Figure captions

Table 1: Observed Raman modes at ambient pressure, their pressure induced frequency shift  $\delta\nu_i$  and Grüneisen parameters  $\gamma_i$  up to 17 GPa.  $\beta$  is the isothermal compressibility coefficient. L or H means the lower or higher frequency branch of the split modes above 6 GPa and below 26 GPa.

Table 2: Luminescence lines (in  $cm^{-1}$ ) of  $LiYF_4 : Pr^{3+}$  at ambient pressure. The assignment of the transitions is given in the irreducible representations  $\Gamma_1$ ,  $\Gamma_2$ ,  $\Gamma_3$  and  $\Gamma_4$  of the  $S_4$  point group. The degenerate  $\Gamma_3$  and  $\Gamma_4$  are denoted by  $\Gamma_{3,4}$ .

Figure 1, Scheelite structure of  $LiYF_4$  with space group  $C_{4h}^6$ .  $Y^{3+}$  ion is coordinated to eight  $F^-$  ligand ions at the corners of the eight  $LiF_4$  tetrahedra around it and has a  $S_4$  or  $D_{2d}$  site symmetry.

Figure 2, Projection of the tetrahedra in a unit cell of the scheelite structure of  $LiYF_4$  on the (001) plane. The full circles represent the eight  $F^-$  ligands of  $Y^{3+}$ .

Figure 3, Pressure influence on the Raman spectra of  $LiYF_4$ . The variation in line intensity of the spectra below 16 GPa is mainly due to the different orientations of the samples during the experiments.

Figure 4, Pressure dependence of the Raman frequency of  $LiYF_4$ . The size of the symbols represents the error of the measurements. The dashed lines are just guides for the eye.

Figure 5, Comparison of the spectra recorded at ambient pressure for  $LiYF_4$  after different treatments: (a) no treatment; (b) sample pressurized to 11 GPa, recorded about 15 minutes after releasing the sample from pressure cell; (c) sample as in (b) but recorded immediately after releasing the sample; (d) sample released from 21 GPa. This spectrum remains different from that of (a) or (b).

Figure 6, pressure dependence of the square of the pressure-induced soft phonon energy. The size of the symbols represents the error of the measurements.

Figure 7: Pressure influence on the luminescence spectra of  $Pr^{3+}$  in  $LiYF_4$ : (a)  $^3P_{0,1} - ^3H_5$  transitions, (b)  $^3P_{0,1} - ^3H_6$  and  $^3P_{0,1} - ^3F_2$  transitions.

Figure 8: Pressure dependence of the fluorescence lines from the transitions (a)  $^3P_0 - ^3H_4$ ; (b)  $^3P_0 - ^3H_5$ ; (c)  $^3P_0 - ^3H_{4,6}$ ,  $^3P_0 - ^3F_2$  and  $^1D_2 - ^3H_{4,6}$ ; and (d)  $^3P_0 - ^3F_2$ ; for  $Pr^{3+}$  in  $LiYF_4$ . The size of the symbols represents the standard error of the measurements. See table 1 for the assignment of the lines L1 to L4.

Figure 9: Emission spectrum recorded at ambient pressure for  $LiYF_4 : Pr^{3+}$  released from 23 GPa.

Table 1,

obs. mode ( $\text{cm}^{-1}$ )	symmetry	$\Delta\nu$ ( $\text{cm}^{-1}$ )	$10^3 \gamma_i \beta$ ( $\text{GPa}^{-1}$ )
153	Eg	-20	-7.26
172	Bg	18	5.81
197	Eg	15	4.23
246	Bg	13	2.94
264	Ag	61	12.84
324(L)	Eg or Bg	28 at 6 GPa and then $\cong 0$	14.4 at 6 GPa
324(H)	Eg or Bg	89	15.26
376(L)	Eg or Bg	57	8.42
376(H)	Eg or Bg	74	10.93
424	Ag and Bg	50 at 6 GPa and then $\cong 0$	19.7 at 6 GPa
444	Eg	6 at 2 GPa	6.76

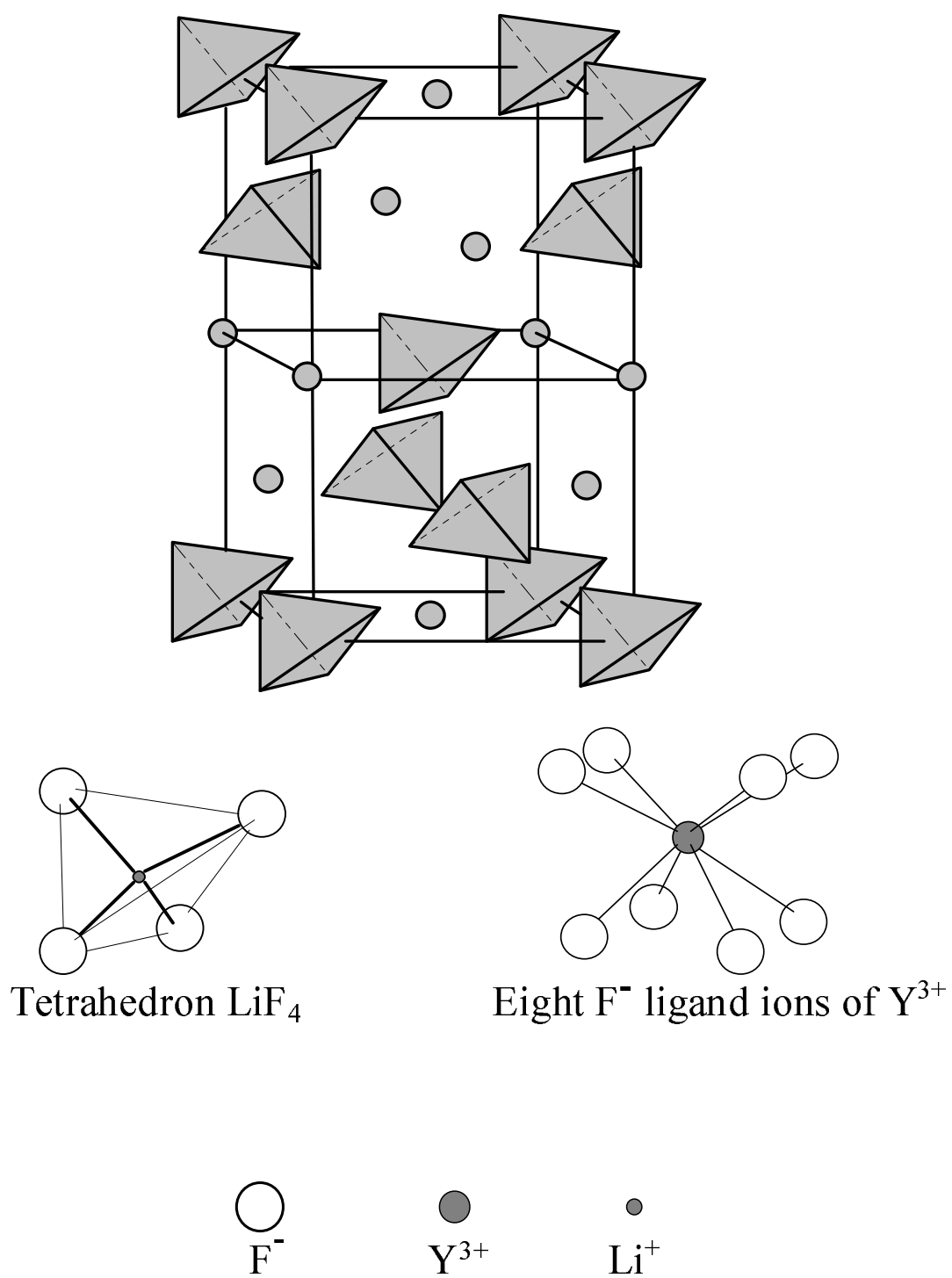


Figure 1, Scheelite structure of  $\text{LiYF}_4$  with space group  $C_{4h}^6$ . The  $\text{Y}^{3+}$  ion has eight  $\text{F}^-$  ligand ions at the corners of the tetrahedra  $\text{LiF}_4$  around it.

**Table 2:**

energy levels (cm <sup>-1</sup> )		<sup>1</sup> D <sub>2</sub> (Γ <sub>2</sub> )	<sup>1</sup> D <sub>2</sub> (Γ <sub>2</sub> )	<sup>1</sup> D <sub>2</sub> (Γ <sub>3,4</sub> )	<sup>3</sup> P <sub>0</sub> (Γ <sub>1</sub> )	<sup>3</sup> P <sub>1</sub> (Γ <sub>3,4</sub> )
		16740±3	16740±3	17094±3	20872±3	21422±3
<sup>3</sup> H <sub>4</sub> (Γ <sub>2</sub> )	0	16740(L <sub>24</sub> )	16820(L <sub>23</sub> )	17094(L <sub>13</sub> )	20872(L <sub>3</sub> )	21422(L <sub>1</sub> )
<sup>3</sup> H <sub>4</sub> (Γ <sub>3,4</sub> )	82±3				20792(L <sub>4</sub> )	21337(L <sub>2</sub> )
<sup>3</sup> H <sub>5</sub> (Γ <sub>2</sub> )	2280±3				18592(L <sub>9</sub> )	19142(L <sub>5</sub> )
<sup>3</sup> H <sub>5</sub> (Γ <sub>3,4</sub> )	2342±3				18527(L <sub>10</sub> )	19082(L <sub>6</sub> )
<sup>3</sup> H <sub>5</sub> (Γ <sub>2</sub> )	2550±1				18322(L <sub>11</sub> )	18872(L <sub>7</sub> )
<sup>3</sup> H <sub>5</sub> (Γ <sub>3,4</sub> )	2672±3				18197(L <sub>12</sub> )	18752(L <sub>8</sub> )
<sup>3</sup> H <sub>6</sub> (Γ <sub>2</sub> )	4325±3				16550(L <sub>16</sub> )	17094(L <sub>13</sub> )
<sup>3</sup> H <sub>6</sub> (Γ <sub>3,4</sub> )	4400±1				16472(L <sub>17</sub> )	17022(L <sub>14</sub> )
<sup>3</sup> H <sub>6</sub> (Γ <sub>3,4</sub> )	4456±2				16417(L <sub>18</sub> )	16964(L <sub>15</sub> )
<sup>3</sup> H <sub>6</sub> (Γ <sub>2</sub> )	4560±1				16312(L <sub>19</sub> )	
<sup>3</sup> H <sub>6</sub> (Γ <sub>3,4</sub> )	4920±1				15952(L <sub>20</sub> )	
<sup>3</sup> F <sub>2</sub> (Γ <sub>3,4</sub> )	5230±0				15642(L <sub>21</sub> )	
<sup>3</sup> F <sub>7</sub> (Γ <sub>2</sub> )	5352±1				15520(L <sub>22</sub> )	